

Mass of ^{59}Zn

B. Sherrill, K. Beard, W. Benenson, B. A. Brown, E. Kashy, and W. E. Ormand
Cyclotron Laboratory and Physics Department, Michigan State University, East Lansing, Michigan 48824

H. Nann, J. J. Kehayias, A. D. Bacher, and T. E. Ward
Indiana University Cyclotron Facility, Bloomington, Indiana 47405
 (Received 29 March 1983)

The ground state Q value of the reaction $^{58}\text{Ni}(p,\pi^-)^{59}\text{Zn}$ has been measured with $E_p = 190$ MeV. The measured Q value was $-144.735(40)$ MeV and the cross section at 30 deg was found to be $0.080(20)$ nb/sr. Also measured was the low-lying level structure of ^{59}Zn and an upper limit on the reaction cross section for $^{40}\text{Ca}(p,\pi^-)$ going to the ground state of ^{41}Ti . The measured mass of ^{59}Zn was used to study Coulomb energy systematics.

[NUCLEAR REACTIONS $^{58}\text{Ni}(p,\pi^-)^{59}\text{Zn}$, $^{40}\text{Ca}(p,\pi^-)^{41}\text{Ti}$, $E_p = 190$ MeV; measured ^{59}Zn mass, low-lying energy levels; calculated ft values, σ . Studied Coulomb energy systematics.

I. INTRODUCTION

The nucleus ^{59}Zn is the heaviest $T_z = -\frac{1}{2}$ nucleus for which the mass and lifetime are known. This makes it important for mass predictions and calculations of Gamow-Teller matrix elements in nuclear beta decay. The mass measurement of ^{59}Zn also represents the first in a

series of $Z > N$ nuclei in this region of the isotope table which are needed to extend the Garvey-Kelson symmetric mass predictions¹ to $A > 56$. Further, since the mass of the $T_z = -\frac{1}{2}$ mirror nucleus is known, the Coulomb energy systematics can be extended to the $A = 59$ mirror pair.

This measurement is the first use of the (p,π^-) reaction to measure a nuclear mass. The (p,π^-) reaction allows a

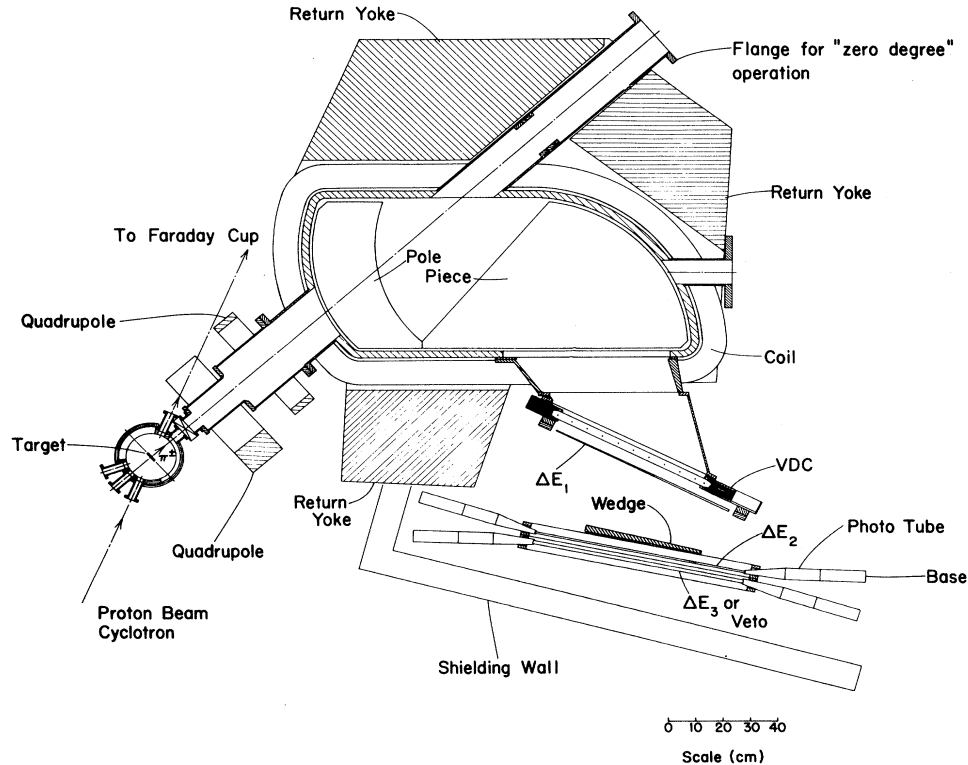


FIG. 1. Overview of the QQSP spectrometer. The aluminum absorbing wedge was used to make the negative pions stop in the ΔE_2 scintillator.

considerably more accurate (< 50 keV) mass measurement and ft -value calculation than the beta-end-point technique commonly used to make mass measurements of proton rich nuclei.

II. METHOD

The measurement was performed at the Indiana University Cyclotron Facility (IUCF) with a proton beam of 190 MeV. The QQSP spectrometer² set at 30 deg was used to determine the outgoing pion kinetic energy. At the focal plane of the spectrometer a vertical drift chamber detector measured both position and angle.³ Figure 1 shows the spectrograph and detector layout. The standard setup, which is described in Ref. 3, uses time of flight between the scintillators and between the front scintillator and the rf of the cyclotron to eliminate background from other particles, particularly electrons. In the present experiment an aluminum absorbing wedge was placed after the focal plane detector and before the scintillators. The thickness of the wedge was chosen to cause the negative pions to stop in the last scintillator, where they deposited some part of their rest mass energy plus their kinetic energy. Thus, by gating on large ($\Delta E_2 > 40$ MeV) energy signals in the ΔE_2 scintillator we were able to reduce the background by two orders of magnitude without changing the efficiency. The limitation of this technique is that it works for only a limited range of pion energy due to the geometry of the wedge and the pion orbits in the spectrograph.

The mass measurement itself was carried out by determining the Q value of the reaction $^{58}\text{Ni}(p,\pi^-)^{59}\text{Zn}$ relative to the Q values of the calibration reactions⁴

$$^{13}\text{C}(p,\pi^-)^{14}\text{O}(\text{g.s.}) \quad Q = -136.650 \text{ MeV},$$

$$^{25}\text{Mg}(p,\pi^-)^{26}\text{Si}(1.796 \text{ MeV}) \quad Q = -140.595 \text{ MeV},$$

$$^{25}\text{Mg}(p,\pi^-)^{26}\text{Si}(2.783 \text{ MeV}) \quad Q = -139.607 \text{ MeV}.$$

Since the QQSP measured angle as well as position, the angular resolution of the detector permitted dividing the ^{14}O calibration runs into 11 0.9-deg angular bins. This gave a calibration point every channel in the region of the ^{59}Zn ground state and provided a precise calibration of spectrograph focal plane. Calibration runs of ^{14}O were taken before and after each ^{59}Zn run to monitor changes in the proton beam energy. The same spectrograph parameters were used for all runs. Finally, the target thicknesses (21.5 mg/cm^2 ^{13}C , 28.5 mg/cm^2 ^{58}Ni , and 26.3 mg/cm^2 ^{25}Mg) were chosen so the energy loss corrections were the same in each target, within 14 keV, for the reactions studied.

III. RESULTS

The Q value for the $^{58}\text{Ni}(p,\pi^-)^{59}\text{Zn}$ reaction was measured to be $Q = -144.735(40)$ MeV, which gives a mass excess of $\text{ME}(^{59}\text{Zn}) = -47.256(40)$ MeV. The measured cross section was $0.080(20)$ nb/sr. This mass compares favorably to the beta-end-point measurement made by Arai *et al.*⁵ of $\text{ME}(^{59}\text{Zn}) = -47.23(10)$ MeV. The weighted average of the two measurements is $\text{ME}(^{59}\text{Zn})$

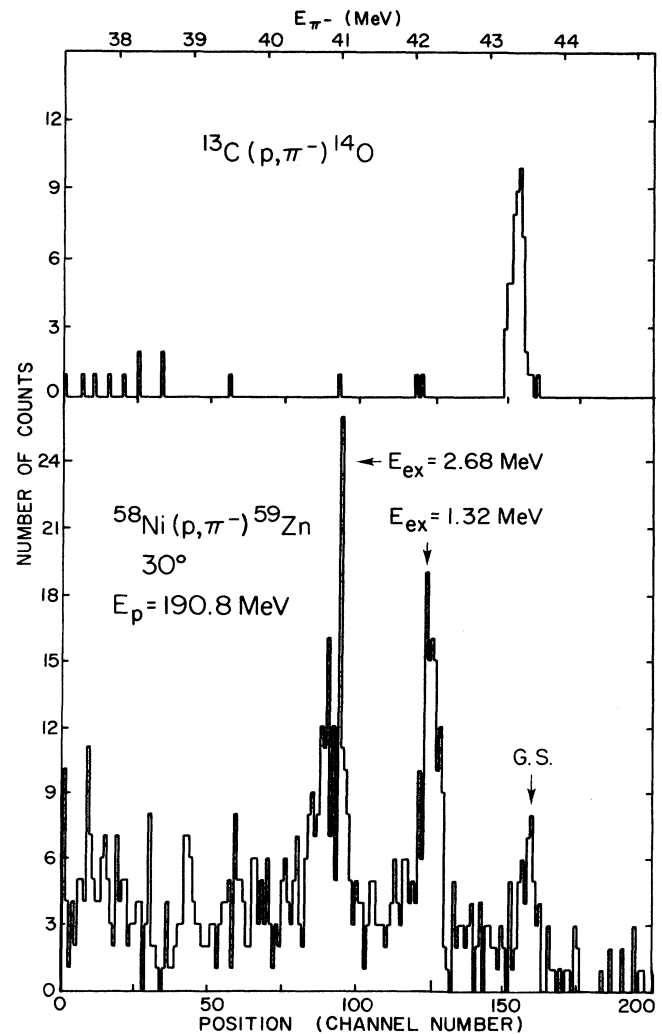


FIG. 2. Position spectra at the focal plane of the QQSP spectrometer, which show the low-lying level structure of ^{59}Zn and a 0.9 deg angular bin of the ^{14}O calibration.

$= -47.253(37)$ MeV. The experimental spectrum is shown in Fig. 2 along with a calibration spectrum. The ^{58}Ni target data are integrated over the whole angular range whereas the ^{13}C spectrum is shown for one of the 0.9 deg angular bins.

The uncertainty in the mass measurement of ^{59}Zn came from four sources. First, the difference in reaction kinematics between $^{58}\text{Ni}(p,\pi^-)$ and the calibration reactions $^{13}\text{C}(p,\pi^-)$ and $^{25}\text{Mg}(p,\pi^-)$ coupled to a 0.5 deg uncertainty in spectrograph angle lead to a 20 keV systematic uncertainty in the measurement. Second, the absolute beam energy was uncertain by 200 keV. This led to a 4 keV uncertainty, again due to the difference in reaction kinematics. Third, beam energy fluctuations observed were of the order of 80 keV. Thus, although the ^{59}Zn runs were shifted and summed according to the observed shifts in the calibration spectra, we conservatively estimated that this fluctuation introduced a 20 keV systematic uncertainty into the mass measurement. Finally, poor statistics,

E_x : (MeV)	J^π	E_x (MeV)	σ (30°) (nb/sr)
2.714	7/2 ⁻	2.68 (8)	0.29(2)
2.709	(5/2 ⁻)		
2.589	(9/2)		
1.988	5/2 ⁽⁻⁾	1.74(6)	0.06(2)
1.865	(7/2 ⁻)		
1.399	7/2 ⁻	1.32(5)	0.21(2)
0.914	5/2 ⁻	0.90(5)	0.04(2)
0.491	1/2 ⁻	0.54(5)	0.03(2)
0.00	3/2 ⁻	0.00	0.08(2)

$^{59}_{29}\text{Cu}_{30}$

$^{59}_{30}\text{Zn}_{29}$

FIG. 3. The measured low-lying level structure of ^{59}Zn compared to the level structure of ^{59}Cu , its mirror nucleus. The ground state energy of ^{59}Zn was shifted to allow comparison of the relative spacing of levels between the ^{59}Zn - ^{59}Cu pair.

due to the small $^{58}\text{Ni}(p,\pi^-)$ cross section and uncertainty in background subtraction, lead to a 28 keV centroid uncertainty. All other contributions to the uncertainty were determined to be less than 4 keV. For the final total uncertainty all effects were added in quadrature.

The measured low-lying level structure of ^{59}Zn is shown in Fig. 3. Also shown is the level structure of ^{59}Cu (Ref. 6), mirror nucleus of ^{59}Zn . The cross sections are consistent with the observation that the (p,π^-) reaction selects high spin states due to the pion-proton momentum mismatch.⁷

The ft values for the β^+ decay of ^{59}Zn have been calculated previously.^{5,9} Using the new mass of ^{59}Zn we obtained a more accurate value for the decay to the ground state ^{59}Cu . The statistical rate function f was calculated, according to the method of Ref. 8, to be $f=25627(848)$. About one-third of the error is from the extension of the parameters in Ref. 8 to all isotopes of a given Z . The remaining error in f is due to the uncertainty of the ^{59}Zn mass. Using the weighted average of the lifetime and branching ratios^{5,9} we obtain $ft=5016(185)$. For this value to be useful for the study of weak interactions the error should be decreased by at least a factor of three. Also of interest are the ft values of the β^+ decays to the excited states in ^{59}Cu . These decays are pure Gamow-Teller transitions. Improvement in their precision might lead to information about weak interactions and nuclear structure effects in weak decays. The main source of error in the decays to the excited states is in the measured values for the branching ratios.

We also attempted to measure the mass of ^{41}Ti with the reaction $^{40}\text{Ca}(p,\pi^-)$, but no counts were observed above the background. This lack of yield gives an upper limit for the cross section of 0.003 nb/sr.

IV. DISCUSSION

Since ^{59}Zn is the heaviest $T_z = -\frac{1}{2}$ nucleus of measured mass it provides a check on the persistence of the Nolen-

Schiffer (NS) anomaly¹⁰ in higher mass nuclei. The measured Coulomb energy shifts between the ^{59}Zn - ^{59}Cu pair are

$$E_c(59;7/2-) = 9810(60) \text{ keV},$$

$$E_c(59;3/2-) = 9882(40) \text{ keV}.$$

We will compare the displacement energies obtained for these $A=59$, $T=\frac{1}{2}$ states with those deduced for other mirror nuclei in the mass range $A=41-55$ and with a standard theoretical model which takes into account the Coulomb interaction between the valence and core nucleons along with some well understood corrections.¹¹ The deviations between experiment and this standard model will be discussed in terms of some conventional improvements which can be made in the model wave functions and in terms of some of the less conventional corrections which have been proposed.

The displacement energy for the $A=59$, $3/2-$ state is calculated by considering this state to consist of a $p_{3/2}$ hole in an $A=60$, $T=0$ closed core. The direct and exchange contributions to the Coulomb matrix elements can be more easily understood by considering the equivalent configuration consisting of three $p_{3/2}$ valence particles in a seniority-one state outside of a ^{56}Ni closed shell. The Coulomb displacement energy is then the sum of the three terms: (d1) the direct term of the interaction between a $p_{3/2}$ proton and the 28 protons in the ^{56}Ni core, (d2) the exchange term for this interaction, and (d3) the Coulomb interaction between the two valence $p_{3/2}$ protons. The exchange term (d2) was taken to be 0.7 times the Fermi gas model prediction [Eq. (3) in Ref. 10]. The factor of 0.7 is based on an average comparison between the exchange terms calculated with harmonic-oscillator wave functions and the Fermi gas model for the $A=15, 17, 39$, and 41 nuclei.^{10,12} The valence two-particle interaction was calculated with a $p_{3/2}$ wave function of seniority one and an harmonic-oscillator radial wave function with an oscillator length deduced from the rms charge radius discussed below.

The direct term (d1) has been calculated numerically with harmonic-oscillator radial wave functions. In order to understand qualitatively how the result depends on the valence (r_v) and core (r_c) point proton rms radii, we have studied several simple functional forms involving these quantities and have found the following result particularly useful

$$\Delta E_d = \frac{6e^2 Z_c}{5R_c(1+\delta/4)}, \quad (1)$$

where

$$R_c = (5/3)^{1/2} r_c,$$

$$\delta = (r_v/r_c)^2 - 1,$$

and Z_c is the number of protons in the core (^{56}Ni in our example). The relative dependence of the exact numerical calculation upon r_c and r_v is well reproduced by ΔE_d , and is in absolute agreement with the exact calculation to within about 0-5% depending on the orbit. The following results for the direct term (d1) will be expressed as the

sum of the contribution from ΔE_d (the term labeled d1a below) and the difference between this and the exact harmonic-oscillator result (the term labeled d1b below). We make use of this division in several ways. First, the finite charge distribution of the proton can be taken into account by replacing R_c in Eq. (1) with the experimental charge radius $R_{ch} = (5/3)^{1/2} r_{ch}$; this also makes it transparent how sensitive the result is to the rms charge radius of the core. Second, we can easily discuss the qualitative model dependence associated with dimensionless quantity δ in Eq. (1). We note that in the limit when the valence and core rms radii are equal ($\delta=0$), ΔE_d is just that for a uniformly charged sphere. In the limit when $r_v \gg r_c$, ΔE_d goes to zero as expected.

The rms charge radius of ^{59}Cu has not been measured, but it can be reliably extrapolated from those measured¹³ in neighboring nuclei as

$$r_{ch}(^{59}\text{Cu}) = r_{ch}(^{58}\text{Ni}) + r_{ch}(^{63}\text{Cu}) - r_{ch}(^{62}\text{Ni}) = 3.822 \text{ fm} .$$

For the total displacement energy we also include: (d4) the relativistic spin-orbit correction [Eq. (21) in Ref. 2], (d5) the vacuum polarization correction [Eq. (4.23) in Ref. 3] and (d6) the contribution from the proton-neutron mass difference [Eq. (4.29) in Ref. 3].

Broken down into the above components the final result for the $A=59$, $p_{3/2}$ state is

$$\begin{aligned} \Delta E(A=59; 3/2-) &= 9.859(1 + \delta/4)^{-1}(\text{d1a}) + 0.219(\text{d1b}) - 0.319(\text{d2}) \\ &+ 0.346(\text{d3}) - 0.036(\text{d4}) + 0.064(\text{d5}) + 0.032(\text{d6}) . \end{aligned}$$

Similarly, the displacement energy for the $A=59$, $7/2-$ state is calculated by considering this state to consist of a $f_{7/2}$ hole in an $A=60$, $T=0$ closed core with the result

$$\begin{aligned} \Delta E(A=59; 7/2-) &= 9.859(1 + \delta/4)^{-1}(\text{d1a}) + 0.014(\text{d1b}) - 0.319(\text{d2}) \\ &+ 0.370(\text{d3}) - 0.107(\text{d4}) + 0.064(\text{d5}) + 0.032(\text{d6}) . \end{aligned}$$

The initial comparisons with experiment will be made by using the harmonic oscillator value $\delta=0.310$ for the $A=59$ states. The ratios of the experimental to theoretical displacement energies are plotted in Fig. 4. In addition we compare in Fig. 4 these ratios for all states in mirror nuclei in the mass region $A=41-55$ which can be considered to be $p_{3/2}$, $f_{7/2}$ or $d_{3/2}$ single-particle or single-hole states outside of $T=0$ core configurations.

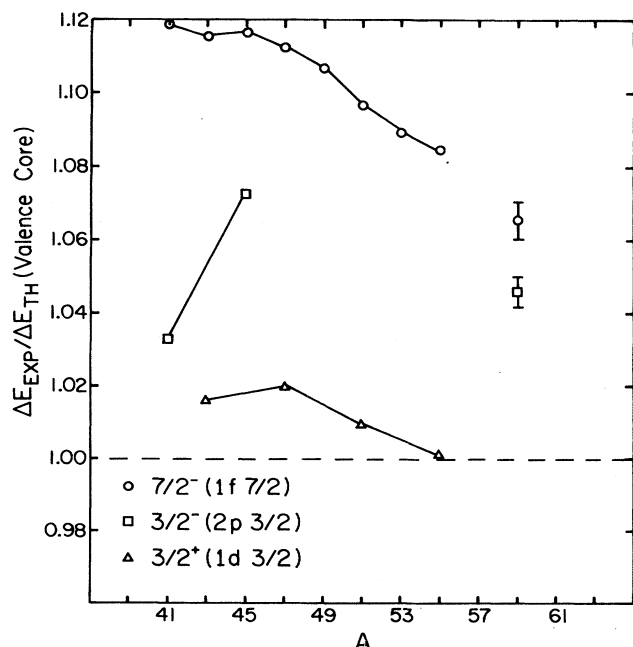


FIG. 4. Ratios of the experimental Coulomb energy differences to those predicted by the valence-core model versus atomic number A .

In the comparison shown in Fig. 4 we immediately notice that for the $A=41$, $7/2-$ state there is an 11% enhancement of experiment over theory which is known as the Nolen-Schiffer anomaly.¹⁰ The ratio for our new $A=59$, $7/2-$ result is consistent with the decrease in the ratio established from the more accurately measured displacement energies in the mass range $A=41-55$.

In $A=41$, the difference between the ratios for the $7/2-$ and $3/2-$ states (see Fig. 4) can be understood as due to the loose binding of the $p_{3/2}$ orbit. With Woods-Saxon radial wave functions the value of $\delta(p_{3/2})$ can become as large as 1.0, compared to the oscillator value of 0.50, thus decreasing the calculated ΔE_d for the $p_{3/2}$ state by about 10% and making the ratios for the $7/2-$ and $3/2-$ states in $A=41$ both about 1.11. [Even though the $f_{7/2}$ orbit in $A=41$ is also rather loosely bound, the larger angular momentum barrier makes the Woods-Saxon and harmonic-oscillator results for $\delta(f_{7/2})$ much more equal.]

In $A=59$ the ratios obtained with the harmonic-oscillator calculations for the $7/2-$ and $3/2-$ states are already much more equal. This is because with increasing mass the $p_{3/2}$ orbit becomes more bound and its radial properties become closer to that for an harmonic oscillator. In addition, we can compare the experimental ratio of 1.007 for $\Delta E(A=59; 7/2-)/\Delta E(A=59; 3/2-)$ to our calculated value of 1.026. I.e., the experimental displacement energies are more similar than those calculated. This orbit dependence in the calculated results, however, could be washed out by configuration mixing expected in more realistic wave functions.

It is interesting to consider the results for the previously known $3/2+$ states shown in Fig. 4 (see the compilations in Ref. 14, Ref. 15 and Ref. 16). Since these $d_{3/2}$ orbits are well bound, the harmonic oscillator is a good approximation. In contrast to the anomaly observed for the fp single-particle states, the $d_{3/2}$ ratio is much closer to uni-

ty. Even though it is mentioned in the original work of Nolen and Schiffer,¹⁰ this dependence of the anomaly on the major shell of the single particle is not widely appreciated.

In Ref. 11 we have shown that this shell dependence, and in fact the entire anomaly, can be explained by the core-compression model proposed by Shlomo and Friedman.^{17,18} Shlomo and Friedman make the hypothesis that the charge radius of both mirror nuclei are equal. Given that the valence radius is in general larger than the core radius, this can only be accomplished by forcing the valence radius to be smaller (the idea originally proposed by Nolen and Schiffer) or by compressing the protons in the proton rich nucleus. Since neither of these effects can easily be reproduced by microscopic calculations, these hypotheses simply shift the displacement energy anomalies into radius anomalies.

Microscopically, the core compression can be calculated as a first-order monopole core-polarization correction to Hartree-Fock theory.¹⁹ We have parameterized the core-polarization corrections calculated with the Skyrme VI interaction in terms of a constant plus a term linear in the parameter δ to obtain (for well bound orbits)

$$\Delta E_{cp} = \frac{6e^2 Z_c}{5R_c} (-0.07 + 0.22\delta).$$

$$r_{ch}({}^{57}\text{Ni}) = r_{ch}({}^{58}\text{Ni}) + r_{ch}({}^{53}\text{Cr}) - r_{ch}({}^{54}\text{Cr}) = 3.753 \text{ fm}.$$

The calculated displacement energy broken down as above is

$$\begin{aligned} \Delta E(A=57; 3/2-) &= 9.986(1 + \delta/4)^{-1}(d1a) + 0.221(d1b) - 0.323(d2) + 0(d3) \\ &\quad - 0.037(d4) + 0.064(d5) + 0.033(d6). \end{aligned}$$

With the oscillator value of 0.310 for δ we then obtain 9.220 MeV. Based on the systematics of the Nolen-Schiffer anomaly shown in Fig. 4 and discussed above, this value should be multiplied by about 1.06 to obtain our prediction for the $A=57, 3/2-$ displacement energy of 9.77 MeV. This displacement energy implies a ${}^{57}\text{Cu}$ ground state mass excess of -47.09 MeV.

The measured mass excess, of ${}^{59}\text{Zn}$, is compared to several mass predictions in Table I. The agreement is typ-

TABLE I. Comparison of mass excess predictions to the measured value.

Mass prediction ^a	Mass excess (MeV)
Myers	-50.4
Grotte-Hilf-Takahashi	-47.73
Seeger-Howard	-48.1
Liran-Zeldes	-47.33
Beiner-Lombard-Mas	-45.8
Janecke-Garvey-Kelson	-47.39
Uno-Yamada ^b constant shell	-47.59
linear shell	-46.87
Experimental value	-47.25(4)

^aS. Maripu, special ed., At. Data Nucl. Data Tables 17, 494 (1976).

^bM. Uno and M. Yamada, Institute for Nuclear Study Univ. of Tokyo Report INS-NUMA-40, 1982, p. 29.

This result is consistent with other calculations of the core polarization.^{20,21} With this correction for the $A=41, 7/2-$ state [with $\delta(f_{7/2})=0.5$] the ratio is reduced from 1.11 (see Fig. 4) to 1.07, and for $A=43$ the $3/2+$ state [with $\delta(d_{3/2})=0.1280$] the ratio is increased from 1.02 to 1.05. For $A=59$ (with $\delta=0.310$) the core-polarization correction is small leaving the ratios unchanged at 1.05 ($3/2-$) and 1.07 ($7/2-$).

Thus, after the core-polarization correction there remains a constant anomaly independent of orbit and mass with the experimental displacement energies to 5–7% larger than those calculated. This may be due to higher order terms left out of the nuclear structure calculations or it may be attributable to a charge symmetry breaking (CSB) interaction (Refs. 12, 21, and for a recent review of CSB see Ref. 22). This we believe is still an interesting and unsolved problem.

At present there is a gap in the experimental mass measurements for mirror nuclei at $A=57$ for ${}^{57}\text{Cu}$ which will probably be soon filled in by new experiments. The ground state spin of ${}^{57}\text{Cu}$ should be $3/2-$ and for this state we can make a prediction for the displacement energy based on a single-particle $p_{3/2}$ configuration outside of a ${}^{56}\text{Ni}$ closed core. The rms charge radius of ${}^{57}\text{Ni}$ can be reliably extrapolated from known radii.^{13,23}

ical for this region of the isotope table. Therefore, there appear to be no surprises in the comparison of the measured mass excess to the mass predictions.

The biggest disadvantage of the use of the (p, π^-) reaction for mass measurements is the small ground state cross section. This is due to the large negative Q values and the resulting proton-pion momentum mismatch. This leads to the selection of high-spin states in the residual nucleus over the usually low-spin ground state. The failure to observe the ground state of ${}^{41}\text{Ti}$ in the ${}^{40}\text{Ca}(p, \pi^-)$ reaction is evidence of this effect. If, however, ${}^{40}\text{Ca}$ had a large 2p-2h neutron component in the ground state, it would show up in the (p, π^-) spectrum. The absence of any observed counts near the expected ground state sets an upper limit of about 25% for the 2p-2h neutron contribution to the ${}^{40}\text{Ca}$ wave function.

Due to the low cross sections and lack of suitable targets there are not many uses for the (p, π^-) reaction in mass measurements. Two remaining possibilities are ${}^{64}\text{Zn}(p, \pi^-){}^{65}\text{Ge}$ and ${}^{92}\text{Mo}(p, \pi^-){}^{93}\text{Ru}$. Many more proton rich nuclei could be reached with the $({}^3\text{He}, \pi^-)$ reaction, but the ground state cross sections are expected to be quite small due in part to a momentum mismatch even worse than that of the (p, π^-) reaction.

The authors are greatly indebted to M. C. Green and the rest of the IUCF pion group for their help on this experiment.

- ¹I. Kelson and G.T. Garvey, *Phys. Lett.* **23**, 689 (1966).
- ²M. C. Green, *Pion Production and Absorption in Nuclei—1981 (Indiana University Cyclotron Facility)*, Proceedings of the Conference on Pion Production and Absorption in Nuclei, AIP Conf. Proc. No. 79, edited by Robert D. Bent (AIP, New York, 1982).
- ³M. C. Green, Ph.D. thesis, Indiana Univ. (unpublished).
- ⁴A. H. Wapstra and K. Bos, 1982 Atomic Mass Evaluation, Nuclear Data Center, Brookhaven National Laboratory (unpublished).
- ⁵Y. Arai *et al.*, *Phys. Lett.* **104B**, 186 (1981).
- ⁶C. M. Lederer and V. S. Shirley, *Table of Isotopes* (Wiley, New York, 1978).
- ⁷B. A. Brown, O. Scholten and H. Toki (unpublished).
- ⁸D. H. Wilkinson and B. E. F. Macefield, *Nucl. Phys.* **A232**, 58 (1974).
- ⁹J. Honkanen *et al.*, *Nucl. Phys.* **A366**, 109 (1981).
- ¹⁰J. A. Nolen, Jr. and J. P. Schiffer, *Annu. Rev. Nucl. Sci.* **19**, 471 (1969).
- ¹¹B. A. Brown and L. Meyer-Schutzmeister (unpublished).
- ¹²S. Shlomo, *Rep. Prog. Phys.* **41**, 957 (1978).
- ¹³E. B. Shera *et al.*, *Phys. Rev. C* **14**, 731 (1976).
- ¹⁴L. Meyer-Schutzmeister *et al.*, *Phys. Rev. C* **18**, 1148 (1978).
- ¹⁵S. A. Gronemeyer *et al.*, *Phys. Rev. C* **21**, 1290 (1980).
- ¹⁶D. Mueller *et al.*, *Phys. Rev. C* **15**, 1282 (1977).
- ¹⁷S. Shlomo and E. Friedman, *Phys. Rev. Lett.* **39**, 1180 (1977).
- ¹⁸E. Friedman and S. Shlomo, *Z. Phys. A* **238**, 67 (1977).
- ¹⁹E. H. Auerbach, S. Kahana and J. Weneser, *Phys. Rev. Lett.* **23**, 1253 (1969).
- ²⁰N. Auerbach, *Nucl. Phys.* **A239**, 447 (1974).
- ²¹J. W. Negele, in *Proceedings of the International Conference on Nuclear Structure and Spectroscopy*, edited by H. P. Blok and A. E. L. Dieperink (Scholars Press, Amsterdam, 1974), p. 618.
- ²²E. M. Henley and G. A. Miller, in *Mesons in Nuclei*, edited by M. Rho and D. Wilkinson (North-Holland, Amsterdam, 1979), Chap. 10.
- ²³H. D. Wohlfahrt *et al.*, *Phys. Rev. C* **23**, 533 (1981).